

Charge-breaking constraints on left-right mixing of stau's

Junji Hisano^{a,b} and Shohei Sugiyama^{a,c}

^a*Department of Physics, Nagoya University, Nagoya 464-8602, Japan*

^b*Institute for the Physics and Mathematics of the Universe, University of Tokyo, Kashiwa 277-8568, Japan*

^c*Department of Physics, University of Tokyo, Tokyo 113-0033, Japan*

Abstract

In the minimal supersymmetric standard model, large left-right mixing of stau's is sometimes intriguing from phenomenological viewpoints. However, too large left-right mixing is not acceptable since the electroweak-breaking vacuum becomes metastable. In this paper the vacuum transition rate is evaluated by using semi-classical techniques, and constraints on parameters of the model are shown. In the calculation the bounce solution is derived in the multifield space. These constraints are also applied to the case of the low-energy minimal gauge mediation model.

1 Introduction

The minimal supersymmetric standard model (MSSM) has two Higgs doublets, and the ratio of their vacuum expectation values, $\tan\beta(\equiv \langle H_u \rangle / \langle H_d \rangle)$, is an important parameter when the phenomenology is discussed. It is expected to be between ~ 2 and ~ 60 if the Yukawa coupling constants for the third generation fermions are perturbative below the GUT scale.

Large $\tan\beta$ is favored from several phenomenological viewpoints. First, the light Higgs boson mass depends on $\tan\beta$ with a high mass at larger $\tan\beta$. The muon $(g-2)$ anomaly also favors large $\tan\beta$ since the SUSY correction is proportional to $\tan\beta$ [1]. Second, the Yukawa unification of the third generation fermions in the SO(10) SUSY GUT requires large $\tan\beta$ [2].

Third, the SUSY CP problem is automatically solved when A and B_μ parameters vanish at high energy scale. The A and B_μ parameters are for trilinear and Higgs bilinear soft-SUSY breaking couplings, respectively. In the case, large $\tan\beta$ is predicted, because $\tan\beta$ is proportional to inverse of the B_μ parameter, while the B_μ parameter is only radiatively generated. It is pointed out in Refs. [3, 4] that in the low-energy minimal gauge mediation (MGM) model, in which the messenger scale is around $10^{(5-6)}$ GeV, $\tan\beta$ is predicted to be $(50 - 60)$. The radiative correction induces tiny B_μ parameter due to the low messenger scale.

Forth, in some gauge mediation models, stau is the next-lightest SUSY particle (NLSP). It is so long-lived that the big bang nucleosynthesis (BBN) may be destroyed [5]. When the left-right mixing term in the stau mass matrix, which is proportional to $\tan\beta$, is large, the annihilation of stau pair is enhanced due to the Higgs s -channel exchange so that the primordial abundance of stau NLSP is reduced [6].

While large $\tan\beta$ sometimes intriguing as mentioned above, it is known that large $\tan\beta$ solutions may suffer from vacuum instability [4]. When the left-right mixing term for stau's is increased, electric charge-breaking minimum in the scalar potential appears and it becomes deeper than the "ordinary" electroweak-breaking minimum. The lifetime of the electroweak-breaking vacuum is required to be longer than the age of the universe.

In this paper, we derive upperbound on the left-right mixing term for stau's as a function of the left- and right-handed slepton masses, by imposing that the electroweak-breaking vacuum has longer lifetime than the age of the universe. The corresponding lowerbound on the stau mass is also shown as a function of the left- and right-handed slepton masses. It is found that the constraints are insensitive to the parameters in the Higgs potential, including $\tan\beta$ itself. When the LHC experiment discovers stau's or gives lowerbound on the mass, the stability of the electroweak-breaking vacuum would be useful to derive the parameters in the stau mass matrix.

The quantum transition rate of the metastable vacuum is estimated by semiclassical technique [7]. We evaluate numerically bounce configuration in three-fields space (left- and right-handed stau's and Higgs boson). The quantum transition rate is evaluated in the previous works, though the bounce configuration is approximated to be one-dimensional

[4, 6]. Thus, our result is more accurate than those.

This paper is organized as follows. In next section, the quantum transition rate of the electroweak-breaking vacuum to the true one is evaluated, and stability of the electroweak-breaking vacuum is discussed. The constraints on parameters for stau mass matrix are derived there. In Section 3 the constraints on the low-energy MGM model are shown. Section 4 is devoted to conclusions and discussion.

2 Stability of vacuum

Stability of the vacuum in the MSSM in the case that $\tan\beta$ is large have been studied in Ref. [4]. In this section we follow their argument and give a more reliable evaluation for vacuum stability.

In gauge mediation models and the constrained MSSM which demands unification of soft scalar squared masses at high scale, sleptons are lighter than squarks because in the former cases slepton masses are proportional to small squared gauge couplings g_Y^2 of $U(1)_Y$ and g_2^2 of $SU(2)_L$ and in the latter case squarks receive large gluino contribution through renormalization group (RG) running. If $\tan\beta$ is large the lightest sfermion is stau for large left-right mixing, which is proportional to the Yukawa coupling of the tau lepton,

$$y_\tau = \frac{m_\tau}{v_d} \sim \frac{\tan\beta}{100}. \quad (1)$$

Too large $\tan\beta$ makes stau tachyonic and classical stability of the electroweak-breaking vacuum is lost. Although the electroweak-breaking vacuum is classically stable, it may be unstable by quantum tunneling effect. If the electroweak-breaking vacuum is not a global minimum but local one in the potential, it would collapse into the global one eventually. Such a metastable vacuum is viable only when its lifetime is longer than the age of the universe.

To see the situation described above in detail we write the scalar potential for neutral component of up-type Higgs H_u , left-handed stau \tilde{L} and right-handed stau $\tilde{\tau}_R$ as follows,

$$V = (m_{H_u}^2 + \mu^2)|H_u|^2 + m_{\tilde{L}}^2|\tilde{L}|^2 + m_{\tilde{\tau}_R}^2|\tilde{\tau}_R|^2 - (y_\tau\mu H_u^*\tilde{L}\tilde{\tau}_R + \text{h.c.}) + y_\tau^2|\tilde{L}^2\tilde{\tau}_R|^2 + \frac{g_2^2}{8}(|\tilde{L}|^2 + |H_u|^2)^2 + \frac{g_Y^2}{8}(|\tilde{L}|^2 - 2|\tilde{\tau}_R|^2 - |H_u|^2)^2 + \frac{g_2^2 + g_Y^2}{8}\delta_H|H_u|^4, \quad (2)$$

where μ is supersymmetric Higgs mass and m^2 's are soft squared masses of each scalar. For simplicity, μ is assumed to be real. Terms including down-type Higgs H_d are ignored since the vacuum expectation value (VEV) is small for large $\tan\beta$. The scalar potential includes an RG-improved term, which is the last term in Eq. (2) and reflects quartic Higgs interaction induced by a loop diagram of the top quark:

$$\delta_H = \frac{3}{\pi^2} \frac{y_t^4}{g_Y^2 + g_2^2} \log \frac{m_{\tilde{t}}}{m_t}. \quad (3)$$

Here, y_t is the Yukawa coupling of the top quark and m_t and $m_{\tilde{t}}$ are the mass of the top and stop, respectively. Typical value of δ_H is ~ 1 . In addition, loop diagrams of the stop also induces the quartic interaction and may make sizable contribution in some cases. It is proportional to A_t^4 , where A_t is an A parameter for stop interaction.

The H_u mass term, $m_{H_u}^2 + \mu^2$, is negative so that H_u gets a VEV v_u . Expanding around this electroweak-breaking vacuum, we have

$$V = m_\phi^2 \phi^2 \left(m_{\tilde{L}}^2 + \frac{g_2^2 - g_Y^2}{4} v_u^2 \right) \tilde{L}^2 + \left(m_{\tilde{\tau}_R}^2 + \frac{g_Y^2}{2} v_u^2 \right) \tilde{\tau}_R^2 - 2y_\tau \mu v_u \tilde{L} \tilde{\tau}_R - 2y_\tau \mu \phi \tilde{L} \tilde{\tau}_R + \frac{g_2^2 - g_Y^2}{2} v_u \phi \tilde{L}^2 + g_Y^2 v_u \phi \tilde{\tau}_R^2 + \frac{m_\phi^2}{v_u} \phi^3 + \dots, \quad (4)$$

where $H_u = v_u + \phi$ and $m_\phi^2 = \frac{g_Y^2 + g_2^2}{2} (1 + \delta_H) v_u^2 = (1 + \delta_H) \sin^2 \beta m_Z^2$. Ellipsis stands for quartic terms. We show only terms with the real parts of scalar bosons in above scalar potential. The first line of Eq. (4) gives a squared mass matrix of stau's,

$$\mathcal{M}_{\tilde{\tau}}^2 = \begin{pmatrix} m_{\tilde{L}}^2 + (\frac{1}{2} - s_W^2) m_Z^2 & \mu y_\tau v_u \\ \mu y_\tau v_u & m_{\tilde{\tau}_R}^2 + s_W^2 m_Z^2 \end{pmatrix}. \quad (5)$$

Here $s_W^2 = g_Y^2 / (g_Y^2 + g_2^2)$ and we take a large $\tan \beta$ limit. Classical stability of the electroweak-breaking vacuum is equivalent to the positivity of the smaller eigenvalue of the matrix $\mathcal{M}_{\tilde{\tau}}^2$.

Even if the classical stability condition is satisfied, the first term in the second line of Eq. (4) could generate a global minimum where $\langle \phi \rangle$, $\langle \tilde{L} \rangle$, and $\langle \tilde{\tau}_R \rangle \neq 0$ and make the electroweak-breaking vacuum metastable.

Quantum transition rate of the metastable vacuum is estimated by semiclassical technique [7]. In this technique the imaginary part of energy of the false vacuum, which is proportional to the transition rate is evaluated using path integral method in Euclidean spacetime. The path integral is dominated by so-called bounce configuration, $\varphi_i = \bar{\varphi}_i(t, \vec{x})$, where $\varphi_1 = \phi$, $\varphi_2 = \tilde{L}$ and $\varphi_3 = \tilde{\tau}_R$ in our case. It is a stationary point of the action and satisfies boundary conditions $\lim_{t \rightarrow \pm\infty} \bar{\varphi}_i(t, \vec{x}) = \varphi_i^f$, where φ_i^f are values of the fields at false vacuum. It is known that we can take an $O(4)$ symmetric solution [8]. The $O(4)$ symmetric Euclidean action is

$$S_E[\varphi(r)] = 2\pi^2 \int dr r^3 \left[\sum_{i=1}^3 \left(\frac{d\varphi_i}{dr} \right)^2 + V(\varphi) \right], \quad (6)$$

where r is a radial coordinate in four-dimensional spacetime. The equation of motion and boundary conditions are

$$2 \frac{d^2 \varphi_i}{dr^2} + \frac{6}{r} \frac{d\varphi_i}{dr} = \frac{\partial V}{\partial \varphi_i}(\varphi), \quad (7)$$

$$\lim_{r \rightarrow \infty} \bar{\varphi}_i(r) = \varphi_i^f, \quad \frac{d\bar{\varphi}_i}{dr}(0) = 0. \quad (8)$$

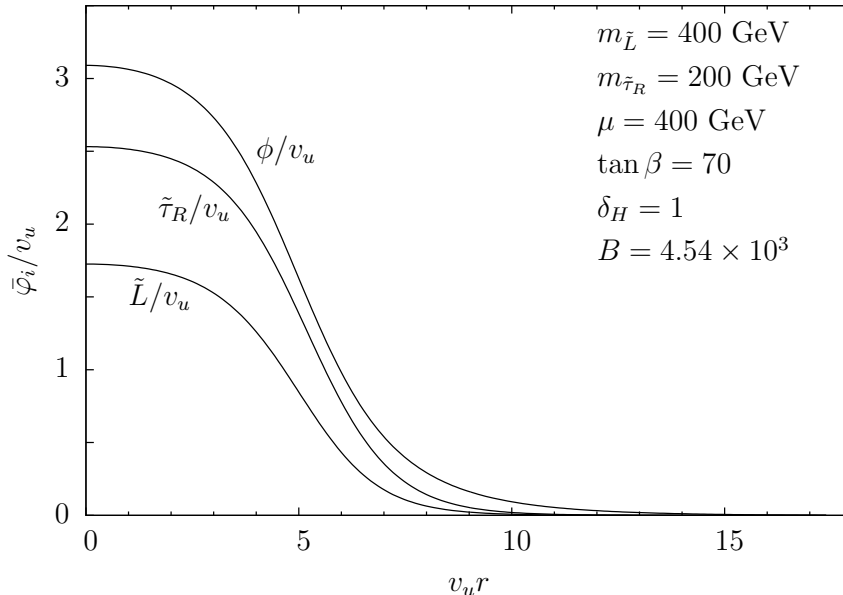


Figure 1: Bounce configuration $\bar{\varphi}_i(r)$ as a function of the radial coordinate r . Parameters of potential and B are shown in figure.

Finally the vacuum transition rate per unit volume is evaluated as follows,

$$\Gamma/V = Ae^{-B}. \quad (9)$$

The prefactor A is the fourth power of the typical scale in the potential. Its precise value is hard to calculate but the transition rate is not sensitive to it. On the other hand, B has an importance in the evaluation and

$$B = S_E[\bar{\varphi}(r)] - S_E[\varphi^f]. \quad (10)$$

If we demand that Γ/V is much smaller than the fourth power of the present Hubble expansion rate $H_0 = 1.5 \times 10^{-42}$ GeV and assume A is $(100 \text{ GeV})^4$, we have constraint on metastability that $B \gtrsim 400$.

For numerical calculation of bounce solutions we used the method of Ref. [9]. Search for bounce solution with single field is easily achieved by overshooting/undershooting method in which one scans initial values $\varphi(0)$ around the global minimum. This scan is difficult in the case of multifield. The authors of Ref. [9] found that in one-dimensional space the initial value $\varphi(0)$ is obtained by using a modified potential. Once we have a bounce solution in one-dimensional space, gradually increasing the spacetime dimension we obtain the four-dimensional solution. Actual calculation is based on a discretized equation of motion.

This method is unsuitable yet to the case that the global minimum is much deeper than local one. Because in that case the modified potential is quite different from original one so that it is difficult to obtain the one-dimensional solution. For such parameter regions,

starting from the solution obtained in region where two minima are nearly degenerate, we gradually change the parameters of the potential and reach the solution.

Fig. 1 is a bounce solution obtained by this method. A trajectory is slightly different from a straight line assumed in Ref. [4]. When $\phi \simeq 0.2v_u$, \tilde{L} and $\tilde{\tau}_R$ approach almost 0.

For the potential of Eq. (4) relevant parameters to vacuum stability are $m_{\tilde{L}}^2$, $m_{\tilde{\tau}_R}^2$, μ , $\tan\beta$ and δ_H . Since the coefficient of quadratic term $\tilde{L}\tilde{\tau}_R$ is proportional to $\mu \tan\beta$ and that of cubic term $\phi\tilde{L}\tilde{\tau}_R$ is nearly proportional to $\mu \tan\beta$, the bounce solution is sensitive to $\mu \tan\beta$, but not $\tan\beta$ itself. To confirm this, we plot contours of B changing $\mu \tan\beta$ and $\tan\beta$ while other parameters are fixed (Fig. 2 (top)). Irrelevance of $\tan\beta$ is clearly seen in the figure. Weak dependence on $\tan\beta$ is generated by the quartic term $y_\tau^2\tilde{L}^2\tilde{\tau}_R^2$ in Eq. (2). This term lifts the global minimum and increases B a little.

Next, we also plot contours changing $\mu \tan\beta$ and δ_H in Fig. 2 (bottom). When A_t is negligible, δ_H mainly depends on the stop mass. If we take $m_{\tilde{t}}$ in the range $600 \text{ GeV} \leq m_{\tilde{t}} \leq 2 \text{ TeV}$, δ_H has the value from 0.65 to 1.3. Larger value of δ_H stabilizes the electroweak-breaking vacuum and slightly increases B . Thus, it is found that the transition rate is sensitive to only $m_{\tilde{L}}^2$, $m_{\tilde{\tau}_R}^2$, and $\mu \tan\beta$ among parameters in the potential of Eq. (4).

In Fig. 3, we show upperbound on $\mu \tan\beta$ that satisfies the metastability condition $B \geq 400$. In numerical calculation we set $\delta_H = 1$ and $\tan\beta = 70$. It is found from Fig. 2 (top) that dependence on $\tan\beta$ changes the result at most 5%. We also evaluate that the dependence on δ_H is less than 1% in the range that $0.65 \leq \delta_H \leq 1.3$. We also show upperbound on $\mu \tan\beta$ that satisfies a rigorous stability condition (the electroweak-breaking vacuum is global minimal in the potential) in Fig. 4. The metastability condition gives about 50% looser constraint on $\mu \tan\beta$ than that the rigorous stability condition.

Upperbound on $\mu \tan\beta$ gives lowerbound on stau mass. We plot stau mass and mixing angle when $\mu \tan\beta$ is taken to be its maximum value allowed by metastability in Fig. 5. Since LEP2 experiments give lowerbounds on stau mass as $m_{\tilde{\tau}_1} \gtrsim 80\text{--}90 \text{ GeV}$ [10], in these region in Fig. 5 the metastability condition gives severer constraint on $\mu \tan\beta$ than the experimental bounds.

We fit this result under the metastability condition to a function as follows,

$$\mu \tan\beta < 76.9\sqrt{m_{\tilde{L}}m_{\tilde{\tau}_R}} + 38.7(m_{\tilde{L}} + m_{\tilde{\tau}_R}) - 1.04 \times 10^4 \text{ GeV}. \quad (11)$$

The difference of this fit is less than 1% in the region where $m_{\tilde{\tau}_1} \gtrsim 80 \text{ GeV}$. This would be useful when considering large left-right mixing of stau's.

3 Application

As an application of the previous section, we consider the low-energy MGM model. The MGM model is the gauge mediation model with a constraint that the B_μ term vanishes at the messenger scale. This model is a solution for the SUSY CP problem in Refs. [3, 4], as mentioned in Introduction.

In this model $\tan\beta$ is an output of the model rather than input. At the tree level, B_μ and $\tan\beta$ are related as follows,

$$-\frac{2B_\mu}{m_{H_u}^2 + m_{H_d}^2 + 2\mu^2} = \sin 2\beta \simeq \frac{2}{\tan\beta}. \quad (12)$$

Since B_μ is generated only through RG running, large $\tan\beta$ is predicted in the low-energy MGM model.

There are two classes of contributions to B_μ . The first one arises from one-loop diagrams of gaugino. The other class is generated by A terms. Since A terms also vanish at the messenger scale, this contribution arises at two loop level. The largest one among A term contributions is proportional to squared Yukawa coupling of the top (or bottom) quark and squared $SU(3)_C$ gauge coupling. Because of these large couplings, the A term contributions are comparable with the gaugino one despite the extra loop. These two contributions have opposite signs, and B_μ is smaller than naive expectation in the low-energy MGM model.

We assume that messengers are $\mathbf{5} + \mathbf{5}^*$ in $SU(5)$ and write couplings to SUSY-breaking sector field S as follows,

$$W = \lambda_T S \bar{q} q + \lambda_D S \bar{l} l, \quad (13)$$

where, q and l are $SU(3)_C$ triplet and $SU(2)_L$ doublet in messenger, respectively. λ 's are coupling constants and S has VEVs $\langle S \rangle = M + \theta^2 F_S$. When λ 's are equal at the GUT scale, they differ at messenger scale due to RG running, which takes λ_T larger than λ_D at low energy. The gaugino masses are expressed as follows,

$$M_i = \frac{\alpha_i}{4\pi} \frac{F_S}{M} g(x_i), \quad (14)$$

where $\alpha_i = g_i^2/4\pi$ and the loop function g is

$$g(x) = \frac{1}{x^2} [(1+x) \log(1+x) + (1-x) \log(1-x)]. \quad (15)$$

$x_{2,3}$ are defined by $x_2 = F_S/\lambda_D M^2$, $x_3 = F_S/\lambda_T M^2$ and $g(x_1) = \frac{2}{5}g(x_3) + \frac{3}{5}g(x_2)$. The difference in λ 's affects the gaugino masses only through the loop function and its effect becomes large in the low-energy MGM model where $F_S \sim M^2$.

In Fig. 6 we show the prediction of the low-energy MGM model and constraints by (meta-)stability of the vacuum. We take $\lambda_D = 1.3\lambda_T$ (top), $\lambda_T = \lambda_D$ (middle), $\lambda_T = 1.3\lambda_D$ (bottom) and $\max(x_2, x_3) = 0.95$. These results are obtained using SuSpect [11] with modification for splitting in couplings of messenger. In the top and bottom figures the ratio of loop functions is $g(0.95) : g(0.95/1.3) = 1.14 : 1$. In gauge mediation models current experimental lowerbound on stau mass is 87.4 GeV [10]. In the case of $\lambda_T = 1.3\lambda_D$, $\tan\beta$ is larger than 60 and the metastability condition gives severer constraint on lower limit of M_2 than experimental lowerbound on stau mass gives. This is explained as follows. In Fig. 6 the magnitude of the A -term contributions to B_μ is larger than that of the gaugino contributions. If $\lambda_T > \lambda_D$, the gluino mass is smaller than the value that GUT relation

is valid. Since leading parts in A -term contribution is proportional to gluino mass, the decrease in gluino mass enhances the cancellation between two classes of contributions. As a result, B_μ becomes smaller at the electroweak scale and larger $\tan\beta$ is predicted. Our result is consistent with those in Ref. [4].

4 Conclusions and discussion

In this paper we have studied vacuum stability constraints on left-right mixing of stau's. $\mu \tan\beta$ is bound by quantum transition to the charge-breaking vacuum. We have shown lowerbound on stau mass from the constraint and its corresponding mixing angle. Our estimation to vacuum transition rate is based on semiclassical technique performed in the three-fields space, which give more precise results than previous works.

We have also considered these constraints in the low-energy MGM model. The vacuum stability conditions constrain parameters of model more severely than experimental limit of stau mass in the case that messenger triplet is heavier than doublet. Such split of couplings in messenger is expected from RG running.

One of issues that we have not handled in this paper is the vacuum transition in the hot universe. The condition that thermal transition to charge-breaking vacuum is suppressed enough would also restrict $\mu \tan\beta$. In addition, electroweak symmetric vacuum should not decay to the charge-breaking vacuum at finite temperature. To trace electroweak-breaking process properly is beyond the scope of this paper and will be studied elsewhere.

Acknowledgment

The work was supported in part by the Grant-in-Aid for the Ministry of Education, Culture, Sports, Science, and Technology, Government of Japan, No. 20244037, No. 2054252 and No. 2244021 (J.H.), and also by the Sasakawa Scientific Research Grant from The Japan Science Society (S.S.). The work of J.H. is also supported by the World Premier International Research Center Initiative (WPI Initiative), MEXT, Japan.

References

- [1] A. Czarnecki and W. J. Marciano, Nucl. Phys. Proc. Suppl. **76** (1999) 245 [arXiv:hep-ph/9810512].
- [2] B. Ananthanarayan, G. Lazarides and Q. Shafi, Phys. Rev. D **44** (1991) 1613; L. J. Hall, R. Rattazzi and U. Sarid, Phys. Rev. D **50** (1994) 7048 [arXiv:hep-ph/9306309]; L. J. Hall and S. Raby, Phys. Rev. D **51** (1995) 6524 [arXiv:hep-ph/9501298].
- [3] M. Dine, Y. Nir and Y. Shirman, Phys. Rev. D **55** (1997) 1501 [arXiv:hep-ph/9607397].

- [4] R. Rattazzi and U. Sarid, Nucl. Phys. B **501** (1997) 297 [arXiv:hep-ph/9612464].
- [5] M. Pospelov, Phys. Rev. Lett. **98** (2007) 231301 [arXiv:hep-ph/0605215].
- [6] M. Ratz, K. Schmidt-Hoberg and M. W. Winkler, JCAP **0810** (2008) 026 [arXiv:0808.0829 [hep-ph]]; M. Endo, K. Hamaguchi and K. Nakaji, arXiv:1008.2307 [hep-ph].
- [7] S. R. Coleman, Phys. Rev. D **15** (1977) 2929.
- [8] S. R. Coleman, V. Glaser and A. Martin, Commun. Math. Phys. **58** (1978) 211.
- [9] T. Konstandin and S. J. Huber, JCAP **0606** (2006) 021 [arXiv:hep-ph/0603081].
- [10] K. Nakamura [Particle Data Group], J. Phys. G **37**, 075021 (2010).
- [11] A. Djouadi, J. L. Kneur and G. Moultaka, Comput. Phys. Commun. **176**, 426 (2007) [arXiv:hep-ph/0211331].

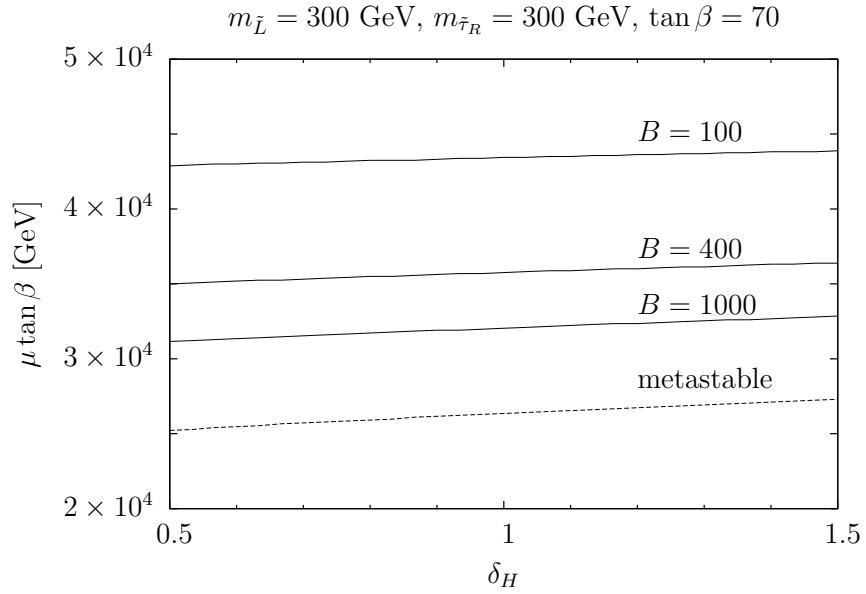
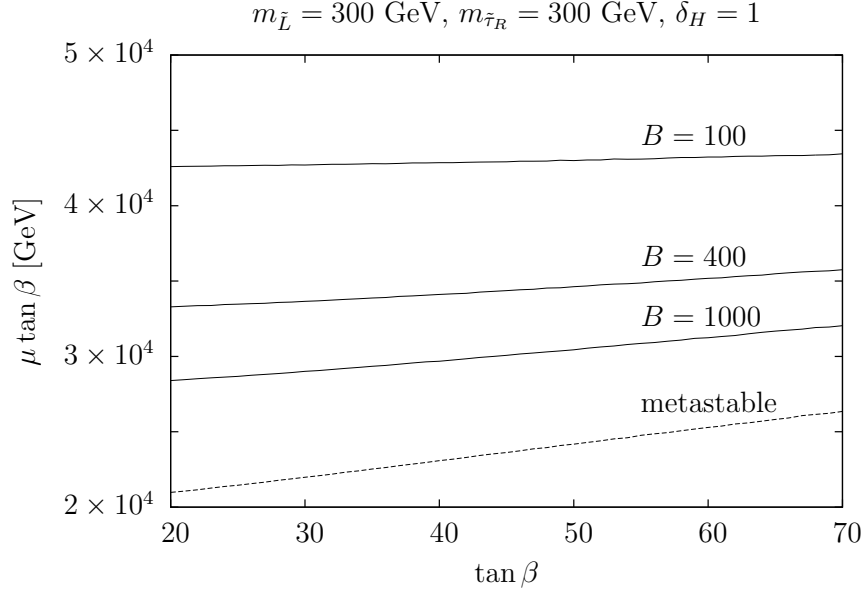


Figure 2: Solid lines are contours of $B = 100, 400$ and 1000 in $\tan \beta - \mu \tan \beta$ plane (top) and $\delta_H - \mu \tan \beta$ plane (bottom). The electroweak-breaking vacuum becomes metastable above broken lines.

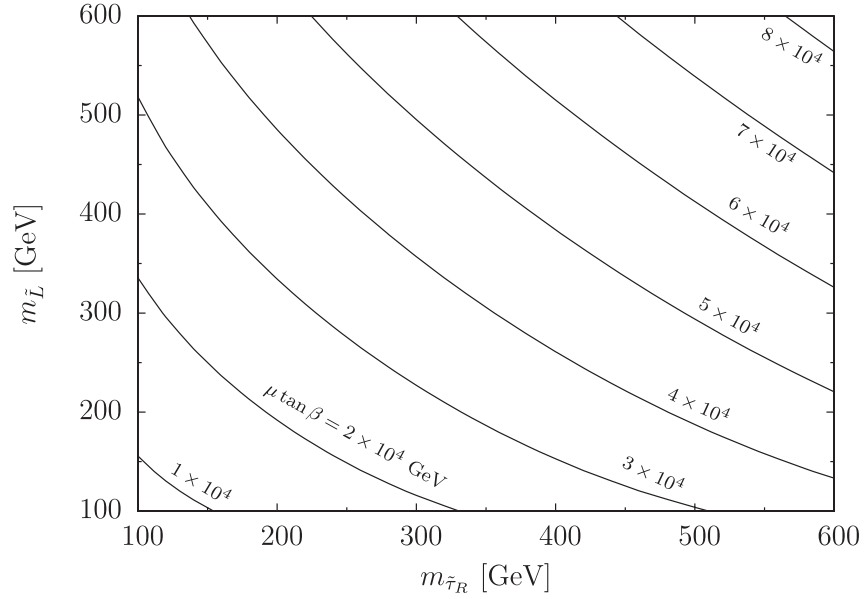


Figure 3: Contour plots for upperbound on $\mu \tan \beta$ that satisfies $B \geq 400$ in $m_{\tilde{\tau}_R} - m_{\tilde{L}}$ plane.

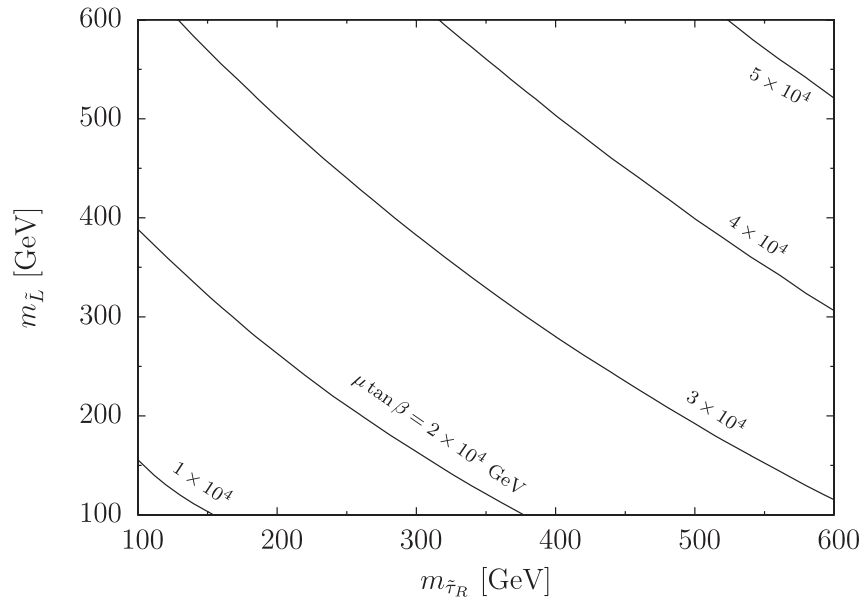


Figure 4: Contour plots for upperbound on $\mu \tan \beta$ that satisfies condition that the electroweak-breaking vacuum is global minimum.

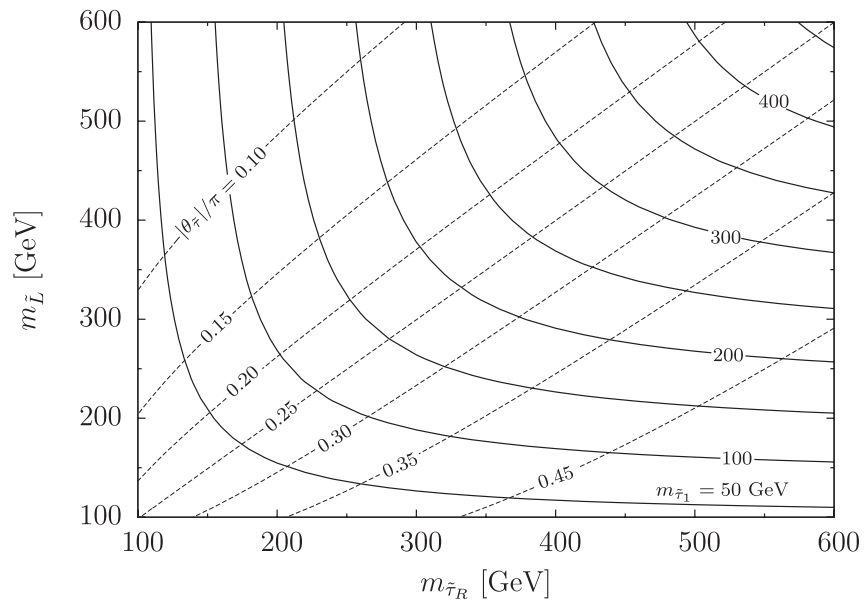


Figure 5: Contour plots for stau mass $m_{\tilde{\tau}_1}$ (solid lines) and stau mixing angle $\theta_{\tilde{\tau}}$ (broken lines) in $m_{\tilde{\tau}_R}-m_{\tilde{L}}$ plane when $\mu \tan \beta$ is taken to be upperbound shown in Fig. 3.

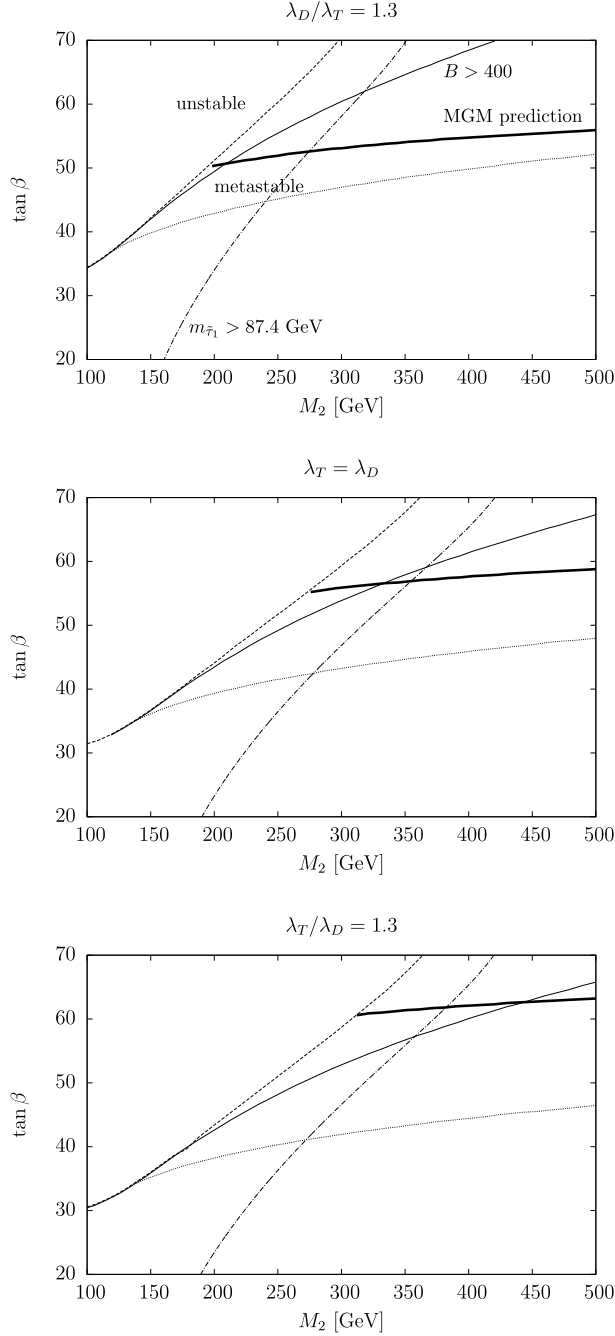


Figure 6: (Meta-)stability constraints in the low-energy MGM model. Horizontal axis corresponds to gaugino mass of $SU(2)_L$, and vertical axis corresponds to $\tan \beta$. Heavy lines indicate predicted value of $\tan \beta$ in MGM. Electroweak-breaking vacuum is unstable above broken lines and metastable above dotted lines. Below solid lines metastability condition $B > 400$ is satisfied. In the right-hand side of dot-dashed lines stau mass is larger than experimental lowerbound. We take $\lambda_D = 1.3\lambda_T$ (top), $\lambda_T = \lambda_D$ (middle), $\lambda_T = 1.3\lambda_D$ (bottom) and $\max(x_2, x_3) = 0.95$ in all cases.